

Performance Investigations of Hybrid Free Space Optics/Radio Frequency (FSO/RF) Links under Turbulence and Misalignment Aperture Error

¹Deepak Kumar Singh and ²Brij Bihari Tiwari

¹Department of Electronics Engineering, VBS Purvanchal University, Jaunpur, U.P. India 222001

²Department of Electronics Engineering, VBS Purvanchal University, Jaunpur, U.P. India 222001

E-mail: ¹deepaksinghaitm641@gmail.com, ²bbitiwari62@gmail.com

ABSTRACT

Free Space Optics (FSO) has played a key role to establish a connection in remote and uncovered skip zone locations. But FSO link performance is degraded due to adverse weather situations and non-line of sight between source and receiver apertures. To improve reliability and reduce losses, a more dependable radio frequency (RF) link can be utilized to backup the FSO link. Hybrid FSO/RF link is considered as a plausible alternative for 5G as well as beyond wireless communication backhaul connectivity. In this study, comprehensive performance investigations of the FSO and single decision-threshold switching assisted hybrid FSO/RF systems have been presented. We consider that the FSO channel follows Gamma-gamma distribution along with atmospheric turbulence as well as pointing errors while, Nakagami-m distribution is used to model RF link fading. We establish the closed-form expressions for average symbol error rate (ASER) as well as outage probability (OP) of the proposed hybrid system with M-ary phase shift keying (M-PSK) and heterodyne detection (HD) schemes. The outcomes of the FSO as well as hybrid systems are validated through Monte-Carlo simulation. A drastic improved in proposed hybrid system performance is reported over the FSO connection under adverse weather situations, pointing errors and atmospheric turbulence due to backup RF connection. At same average SNR value of 50 dB, proposed hybrid model achieves ASER of 10^{-8} without pointing errors, while with pointing errors hybrid model gives ASER of 10^{-7} .

Keywords: Nakagami-m fading, Decision threshold, Free space optics (FSO), Gamma-gamma (GG) distribution, Pointing errors (PE), Average symbol error rate (ASER), Outage probability (OP).

1. INTRODUCTION

To fulfill the higher bandwidth and high speed services demand where wireline (optical fiber cable) solutions and last-mile connectivity problems are difficult to deploy, optical wireless communication (OWC) is the most suited. The concept of OWC is shown in figure (1) as a brief architecture of OWC [1]. OWC is broadly categorized mainly in three forms, visible light communication (VLC) for indoor

applications, ultra-violet non-line of sight (UN-LoS), which is operated at UV frequency for outdoor applications and free space optics communication, which is operated above 100 GHz near infra-red frequency range in Electromagnetic-spectrum. All these OWC technologies have been considered as potential means to fulfill the growing demands of smart hand-held devices, internet of things (IoT) networks and 5G/6G as well as future wireless networks for their special features [2]. Table (1) shows the various technological aspects of OWC technologies.

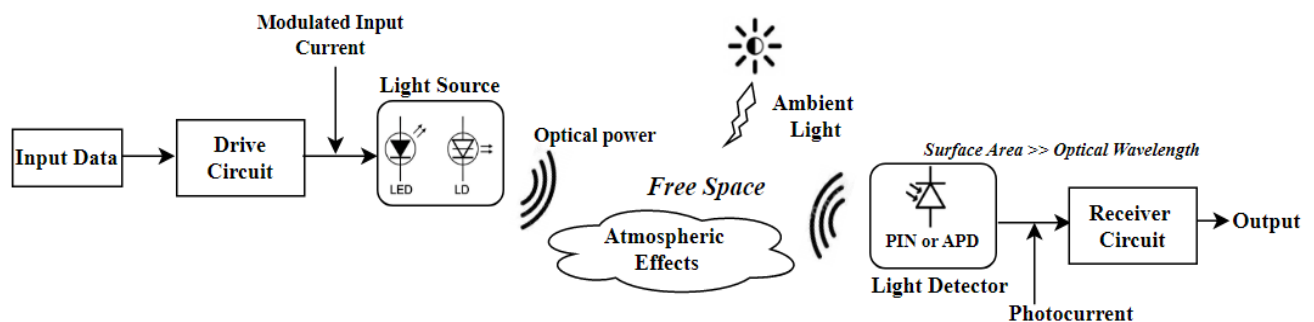


Figure 1: Architecture of Optical wireless communication

Free space optics (FSO) is a revolutionary technology which can satisfy the rising demand for extremely high data rates and enormous bandwidth applications. It provides enormous optical bandwidth, enabling 10 Gbps data rates. FSO employs optical carriers and operates in the unlicensed near-IR spectrum at frequencies exceeding 300 GHz [3]. FSO

communication (700-1600 nm) uses narrow laser beams for data transmission between aligned apertures of transmitter and receiver, i.e., line-of-sight (LoS) communication link, mainly for outdoor applications. Therefore, it is a short distance, low latency, more secure, high bandwidth, high data rate, electromagnetic pollution free unlicensed spectrum and easy is

to deploy. FSO systems are used as backhaul for wireless cellular, Intercampus Connectivity (near terrestrial FSO), satellite-to-ground, satellite to satellite, video surveillance, monitoring and broadcasting live events [4].

Table 1: Various OWC Technologies

OWC Technology	Transmitter (S)	Receiver (S)	Media
VLC	LEDs, ILDs	PDs	Visible light (VL)
Li-Fi	LEDs, Defuse LDs	PDs	VL for forward and IR for reverse path
Optical Camera Communication	Light or LED array	Camera or image sensor	VL, IR and UV
Free Space Optics (FSO)	LDs	PDs or HD	Infra-red, visible light and UV

Fog, snow, and smog are the foremost factors of atmospheric turbulences that degrade FSO transmission performance, making FSO unreliable and limiting FSO transmission to short ranges of a few kilometers. FSO and RF links can be combined as a solution against this challenge. Weather conditions do not have the same impact on FSO and RF connections; for example, fog, atmospheric turbulence, and misaligned aperture errors are the primary causes of FSO link performance deterioration, whereas heavy rain is not. Contrarily, RF is unaffected by fog, snow, and atmospheric turbulences but is vulnerable to heavy rain. As a result, FSO and RF connections are independent from one another and have complementary features [5]. A more reliable RF channel can be utilized as a backup for the FSO link in order to enhance the FSO link's reliability and minimize losses. As a result, both RF and FSO links will cooperate with each other to enhance system performance in adverse weather situations.

The key contributions of this study are as follows:

- In this study, we present a novel single decision threshold switching algorithm assisted hybrid FSO/RF model.
- In hybrid FSO/RF system, the exact closed form equations for outage probability and ASER are established for FSO and RF links.
- We derived the close-form expressions of ASER and outage probability for hybrid system with various M-PSK as well as HD scheme.

Section 2 reviews the earlier works done on performance investigations of hybrid FSO/RF model. The proposed hybrid system and link models as well as statistical-characteristics of RF and FSO links are elaborated in section 3. For the performance evaluation, analytical equations for Outage and ASER are presented in section 4. The simulation results based on analytical equations and discussion are mentioned in section 5. In section 6, the work summary and conclusions are presented.

2. EARLIER STUDIES

A generalized fading channel model i.e., Malaga (M) distribution has been used to model the FSO link in the presence of pointing errors as well as high atmospheric losses in [3]. In addition, the generalized α - η - κ - μ fading model is used to describe RF channel fading along with heterodyne detection (HD) and intensity modulation/direct detection (IM/DD) scheme [3]. The performance of a hybrid FSO/RF system with a hard switching method is explored in [6], wherein a link activation is based on the quality of the FSO connection. A log-normal distribution has been utilized to model weak turbulence of FSO link and Nakagami-m distribution is used to model the RF channel fading [6]. Reference [7] introduced a unique soft switching algorithm for hybrid FSO/RF system based on bit-interleaved coding under adverse weather situations and various turbulence regimes. Moreover, fading of the FSO channel was modeled with Gamma-Gamma distribution. The SER and OP performance of a hybrid FSO/RF model is investigated in Reference [8], wherein, FSO and RF links are considered to be operational every time. Furthermore, at the receiver, both FSO and RF links were mixed using diversity schemes. In [9], a hybrid FSO-RF system alongwith selection-combining (SC) approach has been investigated. Similarly, [10] investigated the hybrid system performance over generalized Malaga (M) distribution with selection-combining scheme. The generalized Malaga (M) distribution can be used to model FSO link fading as Gamma-Gamma and log-normal distributions in special circumstances [11].

Building sway and vibrations induce misalignment between the transmitter and receiver apertures, leading in pointing error deficiencies. The performance of the FSO link has been evaluated in [12, 13, 14], under the influence of pointing errors as well as atmospheric turbulence over log-normal and Gamma-Gamma channel distributions in [13] while, generalized Malaga (M) distributions in [14]. The cooperative diversity approaches were proposed to enhance the system performance and improve the range of the FSO communication. To increase coverage range of FSO link as a last-mile access connection; amplify-and-forward (AF) as well as decode-and-forward (DF) relaying schemes were used with dual-hop mixed FSO/RF models in [15, 16, 17]. In [15], Malaga (M) and Nakagami-m channel distributions are used to model the cooperative DF relaying based hybrid FSO/RF system. While in [16], a dual-hop AF relaying based mixed FSO-RF system has been investigated over milli-meter (mm) wave RF link for backhauling the cellular network.

In [17], a unique DF relaying assisted switching scheme for dual-hop hybrid FSO/RF model is presented, wherein FSO and RF links were coupled at destination using the maximum ratio combining (MRC) approach. The spatial diversity methods like single-input-single-output (SISO), multiple-input-multiple-output (MIMO) have been employed to enhance the system performance in [18, 19]. The spatial diversity MIMO for FSO link alongwith Alamouti space-time block coding approach at the transmitter has been presented in [19]. Generalized Malaga (M) distribution has been employed to model the FSO link fading due to atmospheric turbulence without addressing the impact of pointing errors in [18, 19].

©2012-24 International Journal of Information Technology and Electrical Engineering

Generalized RF link fading distributions have been modeled as α - η - μ , η - μ , κ - μ , and α - κ - μ hybrid models in [20, 21, 22, 23, 24]. These hybrid models have sparked the interest of the research community in recent years owing to their variety of applications and versatility to model diverse RF channel conditions. In [25], a mixed α - η - κ - μ model has been utilized to model RF link fading, which is a novel and highly extensive distribution model.

In this study, a comprehensive performance analysis of hybrid FSO/RF system based on single-threshold assisted switching algorithm is presented under the combined impact of strong atmospheric turbulence, pointing errors as well as path loss. Proposed system utilizes M-ary phase shift keying (PSK) scheme to modulate the information symbols, while heterodyne detection (HD) scheme is employed to recover the baseband information. The Nakagami-m fading distribution is employed to model RF link fading and Gamma-gamma distribution is used to model FSO turbulent link. In proposed hybrid system, the link selection is performed with the help of single decision threshold based switching algorithm. This switching approach is being applied by the authors first time.

3. SYSTEM AND CHANNEL MODELS

In this study, we propose a single decision threshold based switching assisted hybrid FSO/RF model as shown in figure (2), where the instantaneous SNR of the FSO connection determines whether the FSO link or the RF link is active. Both links will be available in parallel and only one of them will be active at a time. Activation of the link will be decided by proposed decision threshold switching algorithm. In the present switching technique, data transmission over FSO links is given a greater priority than data transmission over RF connections, and RF links become active for data transmission when the instantaneous SNR of FSO links drops below γ_{th} - a predetermined threshold SNR. At this instance, a one-bit feedback-signal will be used at the transmitter end to activate the backup RF link.

We consider that the transmitter accurately receives the feedback bit stream without any error and delay as well as the receiver contains perfect channel state information (CSI). In order to modulate the laser beam intensity, we employ sub-carrier intensity modulation based M-ary phase shift keying (SIM-MPSK) signaling at the transmitter end for FSO subsystem [26]. Additionally, the receiver end employs HD method. Moreover, MPSK signaling modulates RF signals.

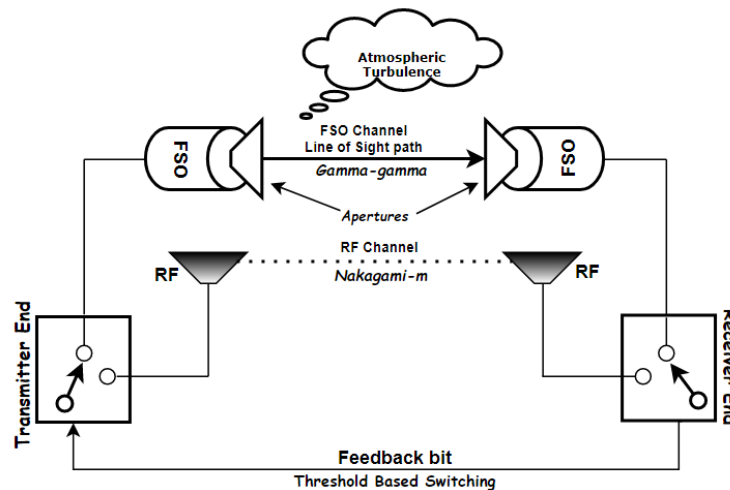
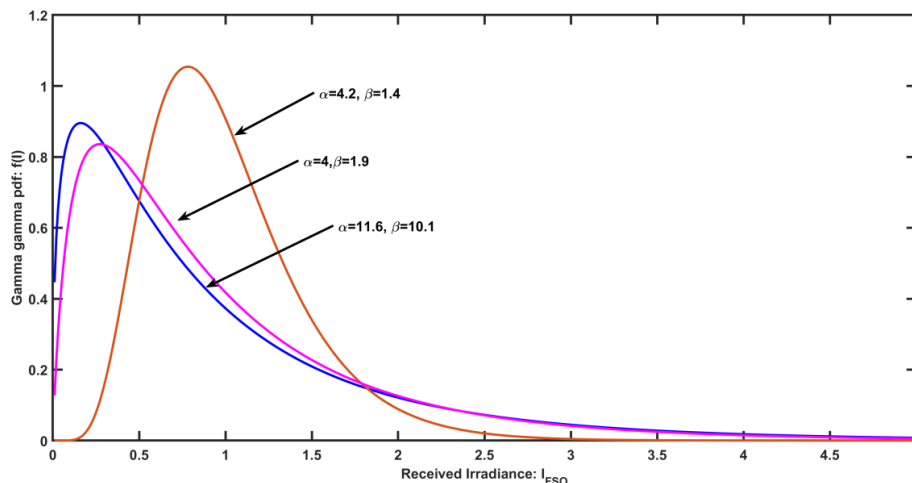


Figure 2: Hybrid FSO/RF model



©2012-24 International Journal of Information Technology and Electrical Engineering

Figure 3: Gamma-gamma PDF with different value of α and β

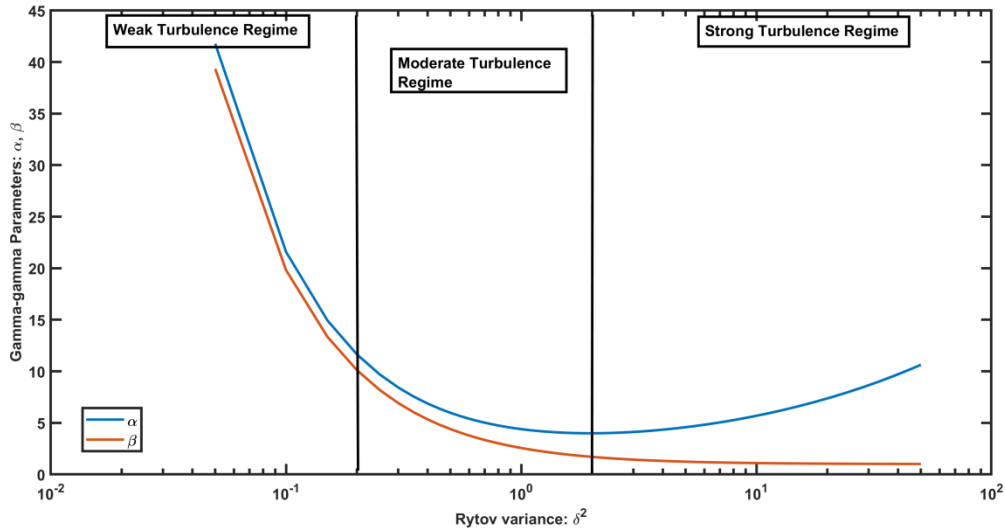


Figure 4: Parameters variation under different turbulence regimes

3.1 FSO SUB-SYSTEM MODEL

We assume Gamma-gamma distribution for modeling the atmospheric turbulence of FSO link. The Gamma-gamma distribution helps to model moderate to strong turbulence regimes. The probability distribution function (PDF) of Gamma-gamma FSO link turbulence model is expressed as [27]

$$f_{I_{FSO}}(I_{FSO}) = \frac{2(\alpha\beta)^{\frac{\alpha+\beta}{2}} I_{FSO}^{\frac{\alpha+\beta}{2}-1} K_{\alpha-\beta}(2\sqrt{\alpha\beta I_{FSO}})}{\Gamma(\alpha)\Gamma(\beta)} \quad (1)$$

where I_{FSO} is the combine channel irradiance of FSO channel, α and β are respectively, the small scale (shape) and large scale factors of scattering situation, $\Gamma(\cdot)$ is the gamma function; $\Gamma(z) = \int_0^\infty x^{z-1} e^{-x} dx$ and $K_\nu(\cdot)$ represents the modified Bessel function of the 2nd kind of order $(\alpha - \beta)$. The parameters α and β are expressed as

$$\alpha = \left[\exp\left(\frac{0.49\delta^2}{(1 + 0.18d^2 + 0.56\delta^{12/5})^{7/6}}\right) - 1 \right]^{-1},$$

$$\beta = \left[\exp\left(\frac{0.51\delta^2(1 + 0.69\delta^{12/5})^{-5/6}}{(1 + 0.9d^2 + 0.62d^2\delta^{12/5})^{5/6}}\right) - 1 \right]^{-1}$$

where $d = \sqrt{kD^2/4L}$; k is wave number ($k = 2\pi/\lambda$), L represents FSO link distance, D is diameter of receiver aperture and λ is optical wavelength. The Rytov variance (δ^2) is related to atmospheric turbulence/scintillation strength (C_n^2) as $\delta^2 = 0.5C_n^2 k^{7/6} L^{11/6}$, which is altitude dependent.

The value of α and β is less as well as δ^2 is large for strong turbulence regimes while the value α and β is large as well as δ^2 is less for weak turbulence regimes. Figure (3) shows the PDF for different value of Gamma-gamma distribution parameters α and β as strong-moderate-weak turbulence regimes. This is a plot between Gamma-gamma distribution parameters α (large-scale eddies) and β (small-

scale eddies) and received irradiance (I_{FSO}) fluctuations. In this study, we consider the FSO link to be in under strong turbulence regimes ($\alpha = 4.2, \beta = 1.4, \delta^2 = 3.5$). Figure 4 shows the Gamma-gamma distribution parameters variations with respect to Rytov variance (δ^2) under different atmospheric turbulence regimes i.e., weak-moderate-strong [2].

The received FSO signal with HD scheme is given by [28]

$$\gamma_{FSO} = P_{FSO}\eta I_{FSO} + n$$

then the instantaneous SNR at the FSO subsystem receiver is expressed as [29]

$$\gamma_{FSO} = \frac{(P_{FSO}\eta I_{FSO})^2}{N_0}$$

where P_{FSO} is transmitted optical power, $N_0/2$ is additive white Gaussian noise variance and η represents responsivity of the photo detector.

Hence the average electrical SNR of the FSO link is expressed as

$$\bar{\gamma}_{FSO} = \frac{(P_{FSO}\eta)^2}{N_0} E[I_{FSO}]^2 = \frac{(P_{FSO}\eta)^2}{N_0}$$

where $E[\cdot]^2 = 1$; $E[\cdot]$ denotes expectation operator.

From FSO channel statistics, using random variable (RV) transformations the instantaneous SNR γ_{FSO} is represented as

$$\gamma_{FSO} = \bar{\gamma}_{FSO} I_{FSO}^2$$

The PDF of the instantaneous SNR γ_{FSO} of the FSO link without pointing error is expressed as [27]

$$f_{\gamma_{FSO}}(\gamma) = \frac{1}{2\Gamma(\alpha)\Gamma(\beta)} \gamma^{-1} G_{0,2}^{2,0} \left(\frac{\alpha\beta\sqrt{\gamma}}{\sqrt{\bar{\gamma}_{FSO}}} \middle| \alpha, \beta \right) \quad (2)$$

where the term $G_q^p \left(z \middle| \begin{smallmatrix} a_p \\ b_q \end{smallmatrix} \right)$ denotes Meijer G-function [30].

The Cumulative distribution function (CDF) of instantaneous SNR γ_{FSO} of the FSO link without pointing error is represented as

$$F_{\gamma_{FSO}}(x) = \int_0^x f_{\gamma_{FSO}}(\gamma) d\gamma$$

$$F_{Y_{FSO}}(x) = \frac{1}{\Gamma(\alpha)\Gamma(\beta)} G_{1,3}^{2,1} \left(\frac{\alpha\beta\sqrt{x}}{\sqrt{Y_{FSO}}} \middle| \begin{matrix} 1 \\ \alpha, \beta, 0 \end{matrix} \right) \quad (3)$$

The FSO link model is considered to include path loss, atmospheric turbulence as well as misalign apertures errors or pointing errors. While, the RF link model includes only path loss and atmospheric fading parameters. Let the atmospheric turbulence, pointing errors and path loss experienced by FSO channel be denoted as I_a , I_p and I_l respectively. Hence the effective and composite link irradiance of FSO channel includes atmospheric turbulence or scintillation, misalign apertures errors or pointing errors as well as path loss factors given by $I_{FSO} = I_a I_p I_l$.

Misalign apertures errors or pointing errors are introduced due to the radial displacement r between detector center and laser beam center i.e., geometric spread. This is modeled using Rayleigh distribution. The amount of collected power at the FSO link receiver aperture of radius a can be represented as [31]

$$I_p \approx A_0 \exp(-2r^2/w_{Leq}),$$

where $A_0 = \text{erf}^2(v)$ is fraction of power received at $r = 0$, $v = \frac{\sqrt{\pi}a}{\sqrt{2}w_L}$ and $w_{Leq} = \frac{w_L^2 \sqrt{\pi} \text{erf}(v)}{2v \exp(-v^2)}$, w_L is Gaussian beam waist, w_{Leq} represents the equivalent beam width and $\text{erf}(\cdot)$ is the error function [32]. Since radial displacement r follows the Rayleigh distribution and applying the RV transformations in above equation, the PDF of misalign apertures errors I_p is expressed as

$$f_{I_p}(I_p) = \frac{g^2}{A_0^2} I_p^{g^2-1}; \quad 0 \leq I_p \leq A_0. \quad (4)$$

where $g = \frac{w_{Leq}}{2\sigma_s}$ is called as pointing error coefficient and σ_s represents standard deviation for jitter.

The atmospheric path loss of an optical link is explored by Beers Lambert Law [31]. Path loss is represented as $I_l = \exp(-\alpha_1 L)$, where α_1 is attenuation coefficient in dB/Km due to adverse weather situations like fog, haze, snow, etc and L is the FSO link distance.

Hence the composite atmospheric channel state of FSO channel including irradiance, path loss and pointing errors is derived as

$$I_{FSO} = I_a I_p I_l \rightarrow I_p = \frac{I_{FSO}}{I_a I_l}; \quad 0 \leq I_p \leq A_0$$

$$0 \leq \frac{I_{FSO}}{I_a I_l} \leq A_0 \rightarrow 0 \leq I_{FSO} \leq A_0 I_a I_l \rightarrow I_a \geq \frac{I_{FSO}}{A_0 I_l}$$

Hence, from conditional probability concept the PDF of I_{FSO} is expressed as

$$f_{I_{FSO}}(I) = \int f_{I_{FSO}/I_a} \left(\frac{I}{I_a} \right) \cdot f_{I_a}(I_a) dI_a$$

$$f_{I_{FSO}}(I) = \int_{I_a = \frac{I_{FSO}}{A_0 I_l}}^{\infty} f_{I_a}(I_a) \frac{f_{I_p} \left(\frac{I_{FSO}}{I_a I_l} \right)}{I_a I_l} dI_a$$

Solving above integral we get the resultant expression of PDF given by

$$f_{I_{FSO}}(I) = \frac{g^2}{\Gamma(\alpha)\Gamma(\beta)} I^{-1} G_{1,3}^{3,0} \left(\frac{\alpha\beta I}{A_0 I_l} \middle| \begin{matrix} g^2 + 1 \\ g^2, \alpha, \beta \end{matrix} \right).$$

The instantaneous SNR of FSO link for HD technique with pointing error is represented by

$$\gamma_{HD} = I_{FSO}^2 \frac{(P_{FSO})^2}{\sigma_{HD}^2}; \quad \text{where } \sigma_{HD}^2 = N_0.$$

The average electrical SNR of FSO link for HD technique including pointing errors is given by

$$\bar{\gamma}_{FSO} = \left(\frac{I_l k A_0 P_{FSO}}{\sigma_{HD}} \right)^2; \quad \text{where } k = \frac{g^2}{g^2 + 1}.$$

since $\gamma_{HD} = I_{FSO}^2 \frac{Y_{FSO}}{(I_l k A_0)^2}$.

Using the power transformation of the RVs, the resultant PDF of FSO link including pointing errors is given by

$$f_{Y_{FSO}}^{PE}(\gamma) = \frac{g^2}{2\Gamma(\alpha)\Gamma(\beta)} \gamma^{-1} G_{1,3}^{3,0} \left(D \frac{\sqrt{\gamma}}{\sqrt{Y_{FSO}}} \middle| \begin{matrix} g^2 + 1 \\ g^2, \alpha, \beta \end{matrix} \right),$$

where $D = \alpha\beta k$.

The CDF of FSO link under pointing error is represented as

$$F_{Y_{FSO}}^{PE}(x) = \frac{g^2}{\Gamma(\alpha)\Gamma(\beta)} G_{2,4}^{3,1} \left(D \frac{\sqrt{x}}{\sqrt{Y_{FSO}}} \middle| \begin{matrix} 1, g^2 + 1 \\ g^2, \alpha, \beta, 0 \end{matrix} \right).$$

Since the instantaneous and average SNRs of FSO link with heterodyne detection (HD) is given by

$$\gamma_{HD} = I_{FSO} \frac{P_{FSO}}{\sigma_{HD}^2}; \quad \bar{\gamma}_{HD} = k A_0 I_l \frac{P_{FSO}}{\sigma_{HD}^2}.$$

Hence, the PDF and CDF of instantaneous SNR of FSO channel for HD scheme are represented as

$$f_{\gamma_{HD}}^{PE}(\gamma) = \frac{g^2}{\Gamma(\alpha)\Gamma(\beta)} \gamma^{-1} G_{1,3}^{3,0} \left(D \frac{\gamma}{\bar{\gamma}_{HD}} \middle| \begin{matrix} g^2 + 1 \\ g^2, \alpha, \beta \end{matrix} \right) \quad (5)$$

$$F_{\gamma_{HD}}^{PE}(x) = \frac{g^2}{\Gamma(\alpha)\Gamma(\beta)} G_{2,4}^{3,1} \left(D \frac{\gamma}{\bar{\gamma}_{HD}} \middle| \begin{matrix} 1, g^2 + 1 \\ g^2, \alpha, \beta, 0 \end{matrix} \right). \quad (6)$$

3.2 RF SUB-SYSTEM MODEL

The received original signal at RF sub-system receiver is given as [3]

$$\gamma_{RF} = \sqrt{P_{RF} g_{RF} h_{RF} x_{RF} + n_{RF}},$$

where h_{RF} represents the small-scale fading-coefficient of the RF link, P_{RF} represents the RF transmitted power, x_{RF} denotes transmitted M-ary PSK signal, n_{RF} represents the AWGN with zero mean and variance $\sigma_{RF}^2 = B_{RF} + N_0 + N_f$. Here, N_f represents noise figure, B_{RF} denotes RF signal bandwidth, and N_0 is spectral density of noise; g_{RF} is average gain of RF link at 60GHz carrier frequency. It is defined by

$$g_{RF} = G_t + G_r - 20 \log_{10} \left(\frac{4\pi L}{\lambda_r} \right) - (\alpha_{oxy} + \alpha_{rain})L,$$

where G_t is transmitter antenna gain, G_r is receiver antenna gain, L represents RF link distance, λ_r denotes RF signal wavelength, α_{oxy} is attenuation due to oxygen absorption, and α_{rain} represents rain absorption attenuation.

In this study, the RF link under the small scale fading is modeled by Nakagami-m distribution. The PDF of RF link is represented by [32]

$$f_{\|h\|}(t) = \frac{2m\Omega_p^{2m-1}}{\Gamma(m)\Omega_p^m} e^{-\frac{m}{\Omega_p}t^2},$$

where $\Omega_p = E[\|h\|^2]$, $\|h\| \geq 0$.

The instantaneous SNR of the RF link is given by

$$\gamma_{RF} = \frac{\|h\|^2 E_s}{N_0},$$

And the average SNR of RF link is given by

$$\bar{\gamma}_{RF} = E \left[\frac{\|h\|^2 E_s}{N_0} \right] = \frac{E_s}{N_0},$$

where $E[\|h\|^2] = 1 = \Omega_p$ and E_s is transmitted RF signal energy.

From RV transformations, the RF channel statistics is expressed as

$$\gamma_{RF} = \|h\|^2 \bar{\gamma}_{RF}; F_{\gamma_{RF}} = \text{Prob.}[\gamma_{RF} \leq x] = F_{\|h\|} \left(\sqrt{\frac{x}{\bar{\gamma}_{RF}}} \right)$$

Hence, the PDF and CDF of RF link is expressed by [33]

$$f_{\gamma_{RF}}(\gamma) = \frac{m^m \gamma^{m-1}}{\Gamma(m) \bar{\gamma}_{RF}^m} e^{-\frac{m\gamma}{\bar{\gamma}_{RF}}},$$

$$F_{\gamma_{RF}}(x) = \frac{x}{\Gamma(m)} \gamma \left(m, \frac{mx}{\bar{\gamma}_{RF}} \right). \quad (7)$$

where $\gamma(a, b)$ represents lower incomplete Gamma function [34].

4. PERFORMANCE ANALYSIS

4.1 OUTAGE PROBABILITY

We derive the closed-form expression of outage probability for the proposed hybrid system over Gamma-gamma distribution channel model in this section. In case of FSO sub-system, when the instantaneous SNR of FSO link drops below the predefined threshold FSO SNR value γ_{th}^{FSO} , then the FSO link declares outage and connection will switch to RF link.

The outage probability (OP) of FSO link without pointing errors is expressed as

$$P_{OP}^{FSO} = \text{Prob.}(\gamma \leq \gamma_{th}^{FSO}) = F_{\gamma_{FSO}}(\gamma_{th}^{FSO}),$$

$$P_{OP}^{FSO} = \frac{1}{\Gamma(\alpha)\Gamma(\beta)} G_{2,1}^{2,1} \left(\alpha\beta \sqrt{\frac{\gamma_{th}^{FSO}}{\bar{\gamma}_{FSO}}} \left| \frac{1}{\alpha, \beta}, 0 \right. \right). \quad (8)$$

When the instantaneous SNR of RF link falls below the predefined threshold RF SNR γ_{th}^{RF} , then the RF link declares outage. The OP of RF link is given as

$$P_{OP}^{RF} = \text{Prob.}(\gamma \leq \gamma_{th}^{RF}) = F_{\gamma_{RF}}(\gamma_{th}^{RF}),$$

$$P_{OP}^{RF} = \frac{\gamma_{th}^{RF}}{\Gamma(m)} \gamma \left(m, \frac{m\gamma_{th}^{RF}}{\bar{\gamma}_{RF}} \right). \quad (9)$$

In case of hybrid system, when the instantaneous SNR of both the links FSO and RF are dropped below γ_{th} - predefined threshold SNR value, then the proposed system will be declared to be in outage. The OP of hybrid system is expressed as

$$P_{OP}^{Hybrid} = F_{\gamma_{FSO}}(\gamma_{th}^{FSO}) \times F_{\gamma_{RF}}(\gamma_{th}^{RF}), \quad (10)$$

The OP of FSO link under pointing errors consideration is given as

$$P_{OP}^{FSO^{PE}} = \text{Prob.}(\gamma \leq \gamma_{th}^{FSO}) = F_{\gamma_{FSO}}^{PE}(\gamma_{th}^{FSO}),$$

$$F_{\gamma_{FSO}}^{PE}(\gamma_{th}^{FSO}) = \frac{g^2}{\Gamma(\alpha)\Gamma(\beta)} G_{2,4}^{3,1} \left(D \sqrt{\frac{\gamma_{th}^{FSO}}{\bar{\gamma}_{FSO}}} \left| 1, g^2 + 1 \right. \right). \quad (11)$$

Similarly, the outage probability of proposed hybrid system with pointing errors is expressed as

$$P_{OP}^{Hybrid^{PE}} = F_{\gamma_{FSO}}^{PE}(\gamma_{th}^{FSO}) \times F_{\gamma_{RF}}(\gamma_{th}^{RF}). \quad (12)$$

Where $F_{\gamma_{FSO}}(\gamma_{th}^{FSO})$ and $F_{\gamma_{RF}}(\gamma_{th}^{RF})$ are the CDF of outage probability of FSO and RF links, respectively.

4.2 AVERAGE SER (ASER)

The average SER of FSO link without pointing errors can be calculated using general form

$$P_e^{FSO} = \int_0^\infty p(e/\gamma) f_{\gamma_{FSO}}(\gamma) d\gamma, \quad (13)$$

Since the conditional probability for M-ary PSK signaling; $p(e/\gamma)$ is given by

$$p(e/\gamma) = \frac{A}{2} \text{erfc}(B\sqrt{\gamma}),$$

where $A = \begin{cases} 1, & M = 2 \\ 2, & M \geq 2 \end{cases}$, and $B = \sin\left(\frac{\pi}{M}\right)$.

Evaluating the integral in Equation (13) and we get

$$P_e^{FSO} = \frac{A 2^{\alpha+\beta-3}}{\pi^{3/2} \Gamma(\alpha) \Gamma(\beta)} \times G_{2,5}^{4,2} \left(\frac{(\alpha\beta)^2}{16B^2 \bar{\gamma}_{FSO}} \left| \frac{1}{2}, \frac{1}{2}, \frac{\alpha}{2}, \frac{\alpha+1}{2}, \frac{\beta}{2}, \frac{\beta+1}{2}, 0 \right. \right). \quad (14)$$

The ASER of proposed hybrid system during non-outage period is given by

$$P_e^{Hybrid} = B_{FSO}(\gamma_{th}) + F_{\gamma_{FSO}}(\gamma_{th}) \times P_e^{RF},$$

where $B_{FSO}(\gamma_{th}) = \int_{\gamma_{th}}^\infty p(e/\gamma) f_{\gamma_{FSO}}(\gamma) d\gamma$; represents the average SER of FSO link during non-outage period.

Similarly, the ASER of RF link is expressed as

$$P_e^{RF} = \int_{\gamma_{th}}^\infty p(e/\gamma) f_{\gamma_{RF}}(\gamma) d\gamma;$$

$$P_e^{RF} = \frac{A}{2} - \frac{AB}{2\sqrt{\pi}} \sum_{l=0}^{m-1} \frac{C^l \Gamma\left(l + \frac{1}{2}\right)}{(B^2 + C)^{l+\frac{1}{2}}}. \quad (15)$$

where $C = \frac{m}{\bar{\gamma}_{RF}}$.

Similarly, the average SER of FSO link including pointing errors is expressed as

$$P_e^{FSO^{PE}} = \int_0^\infty p(e/\gamma) f_{\gamma_{FSO}}^{PE}(\gamma) d\gamma,$$

Evaluating the above integral, the resultant expression of ASER of FSO link including pointing errors is expressed as

$$P_e^{FSO^{PE}} = \frac{A g^2 2^{\alpha+\beta-3}}{\pi^{3/2} \Gamma(\alpha) \Gamma(\beta)} \times G_{4,7}^{6,2} \left(\frac{D^2}{16B^2 \bar{\gamma}_{FSO}} \left| \frac{1}{2}, \frac{g^2+1}{2}, \frac{g^2+2}{2}, \frac{g^2}{2}, \frac{g^2+1}{2}, \frac{\alpha}{2}, \frac{\alpha+1}{2}, \frac{\beta}{2}, \frac{\beta+1}{2}, 0 \right. \right). \quad (16)$$

Similarly, the ASER of proposed decision threshold assisted hybrid FSO/RF system including pointing errors is represented as

$$P_e^{Hybrid^{PE}} = B_{FSO}^{PE}(\gamma_{th}) + F_{\gamma_{FSO}}^{PE}(\gamma_{th}) P_e^{RF}. \quad (17)$$

where $B_{FSO}^{PE}(\gamma_{th}) = \int_{\gamma_{th}}^\infty p(e/\gamma) f_{\gamma_{FSO}}^{PE}(\gamma) d\gamma$; represents the ASER of FSO link with pointing errors during non-outage period.

5. RESULTS AND DISCUSSION

In this section, the unified closed-form expressions as obtained in section 3 and 4 are used to discuss the performance parameters OP and ASER of single FSO link as well as proposed decision threshold switching assisted hybrid FSO/RF model. We use Gamma-gamma distribution to quantitatively describe the strong turbulence regimes for FSO

©2012-24 International Journal of Information Technology and Electrical Engineering

link alongwith pointing errors. Attributes configured for the simulation of FSO, RF links and proposed hybrid systems are listed in Table (2). The Monte-Carlo simulation has been used to validate the outcomes.

Table 2: System Simulation Attributes

Parameters	Values	Specification(s)	
α	2.064	Large-scale parameter	
β	1.342	Small-scale parameter	
m	1	Severity factor of RF	
g	1.75	Pointing error coefficient	
γ_{th}	5 dB	Outage threshold value	
P_{FSO}	40 mW	FSO transmit power	
P_{RF}	10 mW	RF transmit power	
D	0.02 m	Receiver aperture diameter	
M	2,4,8,16	M-ary PSK	
L	1000 m	FSO link distance	
λ	1550 nm	FSO signal wavelength	
η	0.5 A/W	Responsivity	
σ	10^{-14}	FSO noise variance	
σ_S	30 cm	Jitter standard deviation	
$\phi = \phi_A - \phi_B$	$\pi/2$	Phase difference	
Weather dependent parameters of FSO and RF links [3]			
Weather situation	α_{rain} (dB/km)	α_{oxygen} (dB/km)	C_n^2 ($m^{-2/3}$)
Clear air	0	0.43	5×10^{-14}
Light fog	0	4.2	1.7×10^{-14}
Moderate rain	5.6	5.8	5×10^{-15}

In Figures (5) and (6), the outage probability of FSO and RF links are presented using analytical expression found in Equation (8) and (9), respectively. It is observed that for various outage thresholds of 3 dB, 6dB, and 9 dB, the outage probability values are reduced respectively for an average SNR of 50dB.

Figures (7) and (8) show the ASER performance of RF and FSO link respectively, without consideration of pointing error in case of FSO link. In Figure (8), the FSO link has been considered under strong turbulence regime ($C_n^2 = 5 \times 10^{-14} m^{-2/3}$). The BPSK signaling outperforms the 4-PSK, 8-PSK and 16-PSK signaling for the both links. The results show the degradation of ASER performance of both links along with an increment in modulation order. This is because of the increment in phase errors of higher-order modulation schemes under the identical channel conditions. Hence, the BPSK scheme shows the better ASER performance over other PSK schemes. Figures (7) and (8) show the RF link to achieve ASER of 10^{-6} while FSO link achieves ASER of 10^{-8} for same average SNR value of 50 dB.

The ASER performance of decision threshold assisted hybrid FSO/RF system with and without pointing error under strong turbulence regime ($C_n^2 = 5 \times 10^{-14} m^{-2/3}, \alpha = 4.2, \beta = 1.4, \delta^2 = 3.5$) has been shown in Figures (9) and (10), respectively. Plots show that for the same average SNR value of 50 dB hybrid FSO/RF model without pointing errors achieves ASER of 10^{-8} , while with pointing errors hybrid model gives ASER of 10^{-7} . From the plots, it clearly shows the drastic improvement in proposed hybrid system performance under pointing errors impact due to switching techniques benefits. The proposed decision threshold switching assisted hybrid FSO/RF system outperform the single FSO link as well as hybrid FSO/RF system without pointing errors consideration.

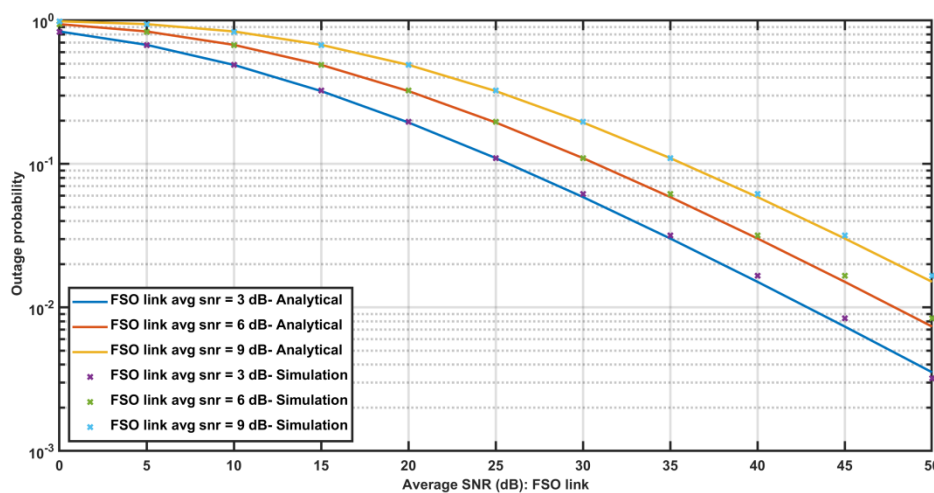


Figure 5: Outage Probability Vs Average SNR of FSO Link

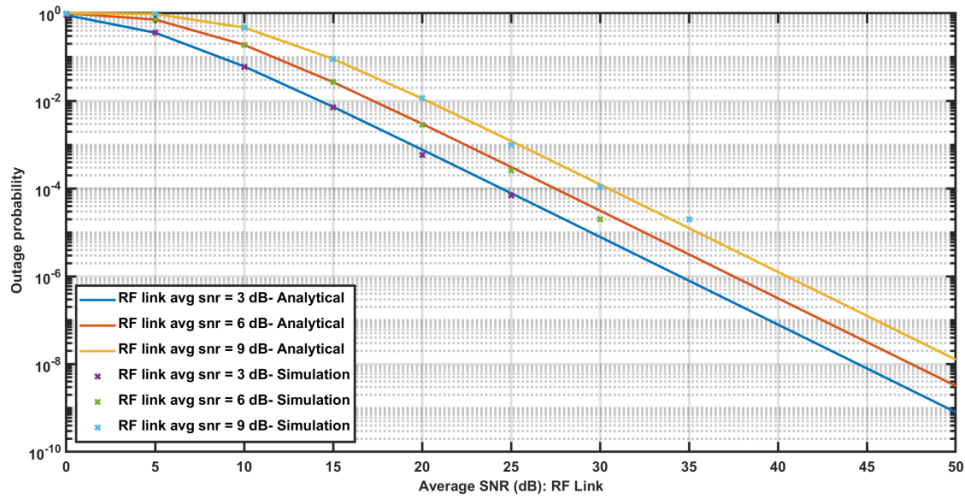


Figure 6: Outage Probability Vs Average SNR of RF Link

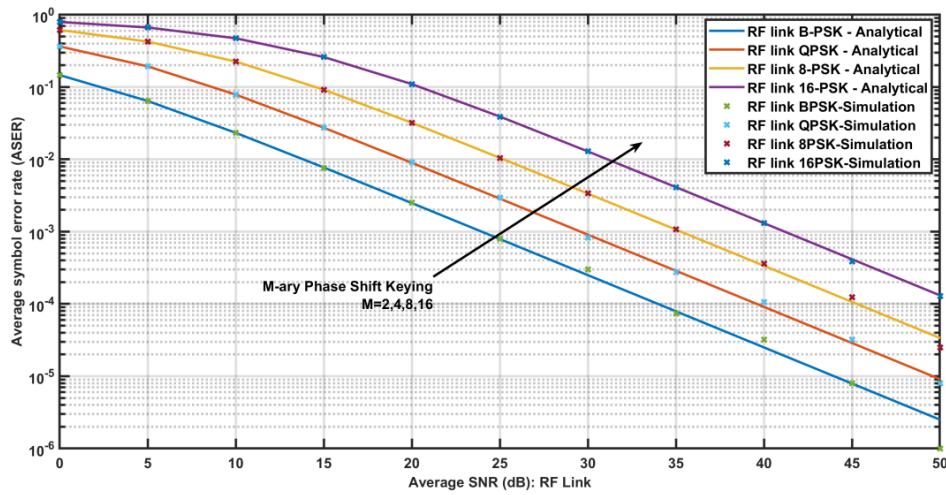


Figure 7: ASER Vs Average SNR of RF Link

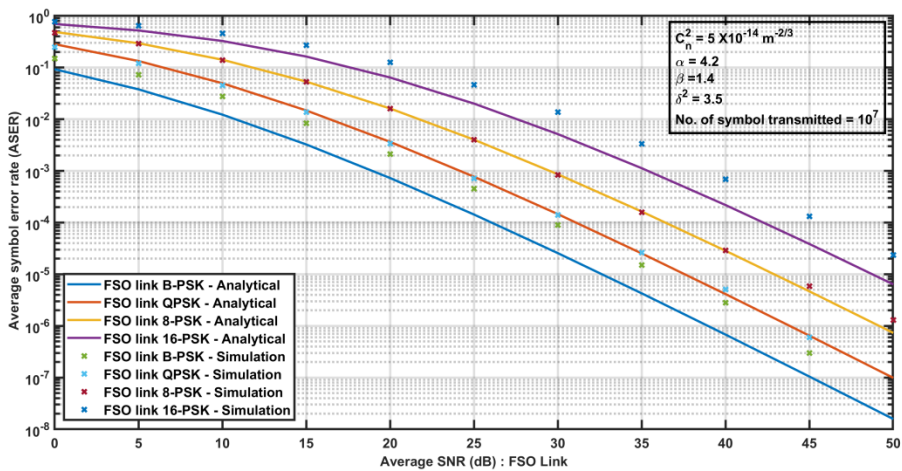


Figure 8: ASER Vs Average SNR of FSO Link without pointing Error

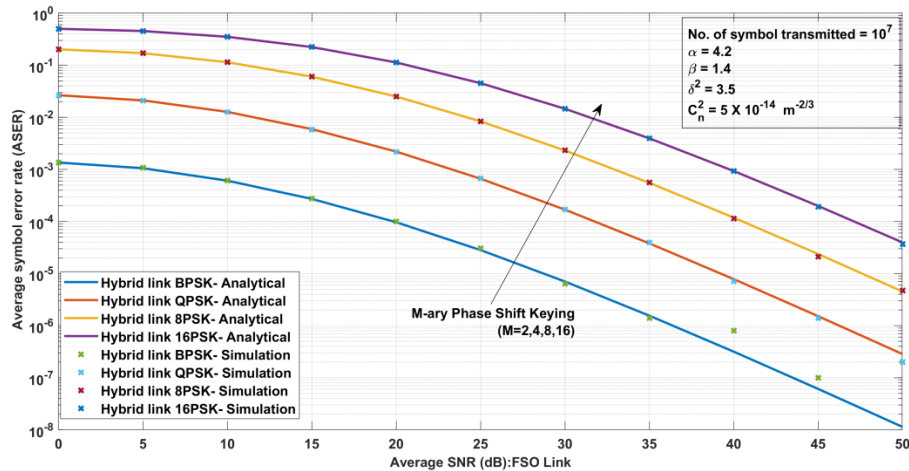


Figure 9: ASER Vs Average SNR of Hybrid FSO/RF system without pointing Error

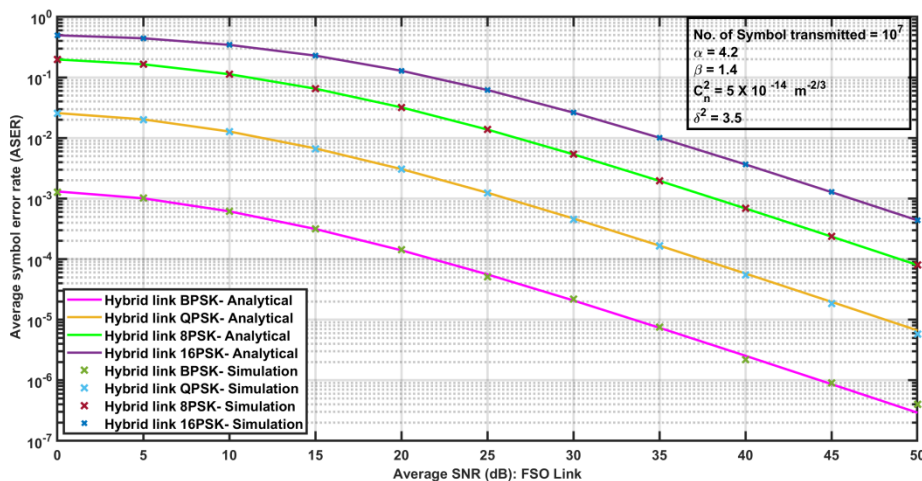


Figure 10: ASER Vs Average SNR of Hybrid FSO/RF system with pointing Error

6. CONCLUSION

A comprehensive performance study of proposed decision-threshold based switching approach assisted hybrid FSO/RF system as well as single RF and FSO links over Nakagami-m and Gamma-gamma fading link model, respectively, has been carried out in the present work. The unified closed-form expressions of the outage probability (OP) and average symbol error rate (ASER) have been computed using the Gamma-gamma distribution for the FSO link and the Nakagami-m fading model for the RF link under various adverse weather situations. Results show that for the same average SNR value of 50 dB hybrid FSO/RF model without pointing errors achieves ASER of 10^{-8} , while with pointing errors hybrid model gives ASER of 10^{-7} . A drastic improvement in proposed hybrid system performance under pointing errors impact due to backup RF link is visible from

the plots. The outage probability results show that the performance of BPSK is superior to that of 4-PSK, 8-PSK and 16-PSK modulation schemes. The proposed decision threshold switching assisted hybrid FSO/RF system outperform the single FSO link as well as hybrid FSO/RF system with perfect channel state conditions.

The study may be further carried on to investigate using generalized channel model such as Malaga (M) distribution for FSO link with spatial diversity techniques such as MIMO, SIMO with MRC to evaluate the performance parameters such as bit error rate, SER, ergodic capacity, secrecy rate, outage probability, channel impulse CDF and link quality of FSO as well as hybrid FSO/RF systems.

REFERENCES

©2012-24 International Journal of Information Technology and Electrical Engineering

- [1] Z. Ghassemlooy, W. Popoola, S. Rajbhandari, "Optical Wireless Communications", CRC Press, T & F Group, 2013.
- [2] C.Y. Li, HH. Lu, C.U. Chou, H.M. Hsia, Y.H. Chen, Y.T. Huang, A. Nainggolan, "A Flexible Bidirectional Fiber-FSO-5G Wireless Convergent System", in Journal of Light Wave Technology, Vol. 39, no. 5, pp. 1296-1305, 2021.
- [3] N. Vishwakarma, R. Swaminathan, "Performance analysis of hybrid FSO/RF communication over generalized fading models", in Journal of Optics Communications, Vol. 487, 2021.
DOI: 10.1016/j.optcom.2021.126796.
- [4] W. Qingqing et al., "Intelligent Reflecting Surface-Aided Wireless Communications: A Tutorial", in IEEE Transactions on Communications, Vol. 69, no. 5, pp. 3313-3351, 2021. DOI: 10.1109/tcomm.2021.3051897.
- [5] M. A. Amirabadi, V. T. vakili, "A novel hybrid FSO/RF communication system with receiver diversity", Journal of Optik, Vol. 184, pp. 293-298, 2019. DOI: 10.1016/j.ijleo.2019.03.037.
- [6] M.K. Simon, M.S. Alouini, "Digital Communications over Fading Channels: A Unified Approach to Performance Analysis", second edition, Wiley-Inter Science, New York, USA, 2005.
- [7] M. Usman, H. Yang, M.S. Alouini, "Practical switching-based hybrid FSO/RF transmission and its performance analysis", in IEEE Photonics Journal, Vol. 6, no. 5, pp. 1-13, 2014.
DOI: 10.1109/JPHOT.2014.2352629.
- [8] B. He, R. Schober, "Bit-interleaved coded modulation for hybrid RF/FSO Systems", in IEEE Transaction on Communication, Vol. 57, no. 12, pp. 3753-3763, 2009.
DOI: 10.1109/TCOMM.2009.12.080396.
- [9] N.D. Chatzidiamantis, G.K. Karagiannidis, E.E. kriezis, M. Matthaiou, "Diversity combining in hybrid RF/FSO systems with PSK modulation", in Proc. IEEE ICC, pp.1-6, 2011. DOI: 10.1109/icc.2011.5962684.
- [10] H. Liang, C. Gao, Y. Li, M. Miao, X. Li, "Analysis of selection combining scheme for hybrid FSO/RF transmission considering misalignment", in Journal of Optics Communication, Vol. 435, pp. 399-404, 2019.
DOI: 10.1016/j.optcom.2018.11.042.
- [11] K.O. Odeyemi, P.A. Owolawi, "Selection combining hybrid FSO/RF systems over generalized induced-fading channels", in Journal of Optics Communication, Vol. 433, no. 8, pp. 159-167, 2019.
DOI: 10.1016/j.optcom.2018.10.009.
- [12] A.J. Navas, J.M.G. Balsells, J.F. Paris, A.P. Notario, "A unifying statistical model for atmospheric optical scintillation", in J. Awrejcewicz (Ed.), Numerical Simulations of Physical and Engineering Processes, Ch. 8, IntechOpen, Rijeka, 2011.
DOI: 10.5772/25097.
- [13] A. Farid, S. Hranilovic, "Outage capacity optimization for free-space optical links with pointing errors", in IEEE/OSA Journal of Lightwave Technology, Vol. 25 no. 7, pp. 1702-1710, 2007.
DOI: 10.1109/JLT.2007.899174.
- [14] F. Yang, J. Cheng, T.A. Tsiftsis, "Free-space optical communication with nonzero bore sight pointing errors", in IEEE Transaction on Communication, Vol. 62, no. 2, pp. 713-725, 2014.
DOI: 10.1109/TCOMM.2014.010914.130249.
- [15] A.J. Navas, J.M.G. Balsells, J.F. Paris, M.C. Vazquez A.P. Notario, "Impact of pointing errors on the performance of generalized atmospheric optical channels", Optical Express, Vol. 20, no. 11, pp. 12550-12562, 2012. DOI: 10.1364/OE.20.012550.
- [16] O.M.S. Al-Ebraheemy, A.M Salhab, A. Chaaban, S.A Zummo, M.S. Alouini, "Precise performance analysis of dual-hop mixed RF/unified-FSO DF relaying with heterodyne detection and two IM-DD channel models", IEEE Photonic Journal, Vol. 11, no.1, pp. 1-22, 2019.
DOI: 10.1109/JPHOT.2018.2890722.
- [17] P.V. Trinh, C.T. Thang, A.T. Pham, "Mixed mm-wave RF/FSO relaying systems over generalized fading channels with pointing errors", in IEEE Photonics Journal, Vol. 9, no. 1, pp. 1-14, 2017.
DOI: 10.1109/JPHOT.2016.2644964.
- [18] S. Sharma, A.S. Madhukumar, R. Swaminathan, "Effect of pointing errors on the performance of hybrid FSO/RF networks", in IEEE Access 7, pp. 131418-131434, 2019. DOI: 10.1109/ACCESS.2019.2940630.
- [19] V. Palliyembil, J. Vellakudiyana, P. Muthuchidambaranathan, "Asymptotic bit error rate analysis of free space optical systems using spatial diversity", in Journal of Optics Communication, Vol. 427, pp. 617-621, 2019.
DOI: 10.1016/j.optcom.2018.07.033.
- [20] A. Das, B. Bag, C. Bose, A. Chandra, "Free space optical links over Málaga turbulence channels with transmit and receive diversity", in Journal of Optics Communication, Vol. 456, 2017.
DOI: 10.1016/j.optcom.2019.124591.
- [21] M.D. Yacoub, "The κ - μ distribution and the η - μ distribution", in IEEE Antennas Propagation Magazine Vol. 49, no. 1, pp. 68-81, 2007.
DOI: 10.1109/MAP.2007.370983.
- [22] J.M. Moualeu, D.B. Costa, W. Hamouda, U.S. Dias, R.A.A Souza, "Performance analysis of digital communication systems over α - κ - μ fading channels", in IEEE Communication Letters, Vol. 23, no. 1, pp. 192-195, 2019. DOI: 10.1109/LCOMM.2018.2878218.
- [23] J.F. Paris, "Outage probability in η - μ / η - μ and κ - μ / η - μ interference-limited scenarios", in IEEE Transaction on Communication, Vol. 61, no. 1, pp. 335-343, 2013.
DOI: 10.1109/TCOMM.2012.092612.110746.
- [24] K.P. Peppas, "Sum of non-identical squared κ - μ variants and applications in the performance analysis of diversity receivers", in IEEE Transaction on Vehicular Technology, Vol. 61, no. 1, pp. 413-419, 2012.
DOI: 10.1109/MAP.2007.370983.
- [25] J.M. Moualeu, D.B. Costa, F.J. Lopez-Martinez, R.A.A. Souza, "On the performance of α - η - κ - μ fading channels", in IEEE Communication Letters, Vol. 23, no. 6, 967-970, 2019.
DOI: 10.1109/LCOMM.2019.2910526.

©2012-24 International Journal of Information Technology and Electrical Engineering

- [26] H. Kaushal, V.K. Jain, S. Kar, "Free Space Optical Communication", Springer, India, 2017.
- [27] D. Singh, B.B. Tiwari, "ASER Performance Analysis of Decision Threshold-Based Hybrid FSO/RF Turbulent Link", in Proceedings of Trends in Electronics and Health Informatics, Lecture Notes in Networks and Systems, Vol. 376, Springer Singapore, 2022. DOI: 10.1007/978-981-16-8826-3_54.
- [28] N. Letzepis, K. Nguyen, A.G. Fabregas, W. Cowley, "Outage analysis of the hybrid free space optical and radio frequency channel", in IEEE J. Sel. Areas of Communication, Vol. 27, no. 9, pp. 1709-1719, 2009.
- [29] S.A. Gailani, M.Z.M. Salleh, A.A. Salem, R.Q. Shaddad, U.U. Sheikh, N.A. Algeelani, T.A. Almohamad, "A Survey of Free Space Optics (FSO) Communication Systems, Links and Networks", in IEEE Transaction on Communication, Vol. 9, 2021.
- [30] Meijer G-function, 2001, <https://functions.wolfram.com/HypergeometricFunctions/MeijerG/>
- [31] A. Farid, S. Hranilovic, "Outage capacity optimization for free-space optical links with pointing errors", IEEE/OSA J. Light wave Technology, Vol.25 no. 7, pp. 1702-1710, 2007. DOI: 10.1109/JLT.2007.899174.
- [32] N Vishwakarma, R. Swaminathan, "On the Capacity Performance of Hybrid FSO/RF System with Adaptive Combining over Generalized Distributions", in IEEE Photonic Journal, Vol. 14, no. 1, 2021. DOI: 10.1109/JPHOT.2021.3135115.
- [33] I.S. Gradshteyn, I.M. Ryzhik, "Table of Integrals, Series, and products", seventh edition, Academic, 2007.
- [34] R. Swaminathan, S. Sharma, N. Vishwakarma, A.S. Madhukumar, "HAPS-based Relaying for Integrated Space-Air-Ground Networks with Hybrid FSO/RF Communication: A Performance Analysis", in IEEE Transactions on Aerospace and Electronic Systems, Vol. 57, no. 3, 2021. DOI: 10.1109/TAES.2021.3050663.

AUTHOR PROFILES

Deepak Kumar Singh received B Tech and M Tech degrees in Electronics & Communication Engineering from Uttar Pradesh Technical University, Lucknow, UP, India. Currently he is pursuing his Ph. D. study in the area of Free Space Optics and design of hybrid FSO/RF system from the Department of Electronics Engineering, VBS Purvanchal University, Jaunpur, UP, India. His current research interest focuses on the design and analysis of hybrid free-space optics/radio frequency communication systems, performance analysis of optical wireless communication systems over generalized fading models, next-generation terrestrial systems, etc. He has attended and published number of research work in reputed journals/IEEE conference/proceedings. He is graduate member of IEEE and IEEE Photonics Society.

Prof. B B Tiwari received the M Sc (Physics) and M Tech (E & C Engineering) degrees from the University of Roorkee (now IIT, Roorkee), India and Ph. D. from the University of Lucknow in 1984, 1986 and 1993, respectively. He is Professor of Electronics Engineering specializing in Photonics and Optical Communication. He has published research papers in reputed journals of the world and has been supervising Ph. D. scholars in the area of optical Communication, Wireless Communication and VLSI Technology. He is Fellow of the Institution of Engineers IE (I) and Fellow of the Institution of Electronics & Telecommunications Engineers IETE (I), India.